The influence of short-range attractive and repulsive interactions on the phase behaviour of model colloidal suspensions

1997 J. Phys.: Condens. Matter 9 8907

(http://iopscience.iop.org/0953-8984/9/42/007)

J. Phys.: Condens. Matter **9** (1997) 8907–8919. Printed in the UK PII: S0953-8984(97)85151-X

The influence of short-range attractive and repulsive interactions on the phase behaviour of model colloidal suspensions

A R Denton†§ and H Löwen†‡

† Institut für Festkörperforschung, Forschungszentrum Jülich, D-52425 Jülich, Germany
‡ Institut für Theoretische Physik II, Universität Düsseldorf, D-40225 Düsseldorf, Germany

Received 13 June 1997

Abstract. The phase behaviour of simple systems interacting via model pair potentials that include both a hard core and additional short-range interactions is predicted using a classical density-functional-perturbation theory. The combination of a narrow attractive square well and a repulsive square barrier, approximating interactions in charge-stabilized colloidal suspensions, gives rise to isostructural solid–solid transitions whose stability is *enhanced* relative to that of the square-well potential alone. The temperature dependence of rms particle displacements for these idealized systems is shown, from both theory and Monte Carlo simulation, to behave anomalously at densities for which neighbouring barriers overlap.

1. Introduction

The stable state of the hard-sphere solid, at all densities beyond freezing, is known from computer simulations [1] and experiments [2] to be a single close-packed (fcc or hcp) crystal. The addition of short-range interactions beyond the hard core, however, can profoundly influence the high-density phase behaviour. As clearly demonstrated by a variety of simulation and theoretical studies [3–13], either attractive *or* repulsive interactions, if of sufficiently short range, may induce a first-order phase transition between two crystals of the same structure below a critical temperature [14]. Although analogous to the more familiar vapour–liquid transition in systems with long-range attraction, this isostructural transition occurs entirely within the solid and is stable (relative to the fluid–solid transition) for attractions or repulsions only of very short range compared with the hard-core diameter.

This remarkable behaviour has been predicted, in particular, for systems interacting via model pair potentials consisting of a hard core plus a narrow attractive square well [3, 4] or repulsive square shoulder [5–9]. Similar behaviour has been predicted for the hard-sphere/attractive-Yukawa system [10, 11] and a class of continuous attractive-well pair potentials [12]. Aside from their fundamental utility in helping to illuminate links between microscopic interactions and macroscopic properties, such extreme pair potentials are also of practical interest as approximate models of the interactions in certain colloidal systems. For example, mixtures of uncharged hard-sphere colloids and non-adsorbing polymers exhibit effective attraction, due to polymer depletion, that is reasonably modelled by a simple square-well potential of width related to the polymer radius of gyration. Suspensions of

§ E-mail: a.denton@fz-juelich.de.

0953-8984/97/428907+13$19.50

uncharged hard-sphere colloids with adsorbed polymers can be similarly approximated by a shouldered potential, although here a simple square shoulder is certainly an extreme idealization.

Despite intriguing predictions, isostructural solid–solid transitions in colloidal suspensions have thus far defied experimental observation. Possible explanations are destabilization by polydispersity [15, 16] and pre-emption by gelation in concentrated suspensions whose van der Waals attraction diverges near hard-core contact [17]. This motivates the present work, the primary purpose of which is to investigate the phase behaviour of a simple system whose interactions include *both* short-range attraction *and* repulsion. Specifically, we focus on a model pair potential combining a hard core, an attractive square well, and a repulsive square barrier. Despite its idealized form, this pair potential does include the major short-range features of the effective pair interactions between sterically and charge-stabilized colloidal suspensions [2, 18, 19], namely a steeply repulsive core, an attractive well, and a repulsive barrier. Applying a practical perturbation theory scheme, previously proven for the square-well [4] and square-shoulder [8] systems, we compute the free energy as a function of density and temperature and thereby predict phase behaviour. The essential qualitative prediction to emerge is that adding a square-barrier interaction to the square-well potential significantly *enhances* the stability of isostructural solid–solid transitions. In addition, we compute, by means of both theory and Monte Carlo simulation, root mean square (rms) displacements of particles from their lattice sites in the solid and examine the variation with temperature and density. For densities such that nearest-neighbour barriers overlap, rms displacements are shown to exhibit anomalous dependence on temperature, *decreasing* with increasing temperature.

We proceed in section 2 by describing our theoretical and simulation approaches, based on classical density-functional theory and the standard Metropolis Monte Carlo algorithm. Section 3 presents our results, in the form of phase diagrams and rms displacements, for the square-well and square-barrier systems alone, as well as for the combined square-well–barrier interaction. Possible relevance to colloidal suspensions is discussed in parallel. Finally, in section 4 we summarize and conclude.

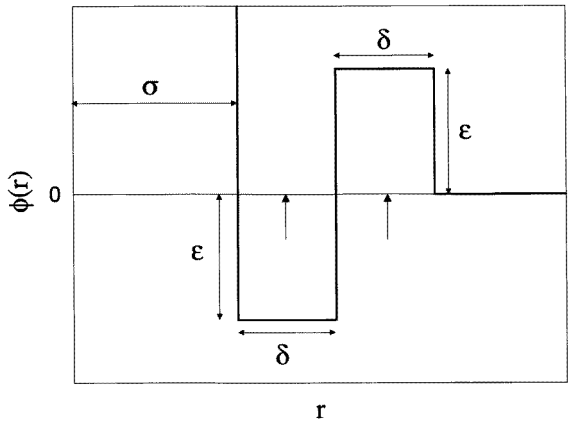

Figure 1. The model pair potential, consisting of a hard core of range σ, a square well, and a square barrier of equal width δ and depth/height ε. The arrows on the horizontal axis indicate nearest-neighbour distances for densities corresponding to figures 2–4(b).

2. Theory and simulation

2.1. Density-functional-perturbation theory

We consider a simple classical system interacting via the model pair potential $\phi(r)$ shown in figure 1, which comprises a hard core of diameter σ, an attractive square well of width δ and depth ε, and a repulsive square barrier of width δ and height ε:

$$\phi(r) = \begin{cases} \infty & r < \sigma \\ -\varepsilon & \sigma < r < \sigma + \delta \\ \varepsilon & \sigma + \delta < r < \sigma + 2\delta \\ 0 & r > \sigma + 2\delta. \end{cases} \tag{1}$$

With temperature and number density measured in units of ε/k_B and σ^{-3}, respectively, the system is completely specified by the single dimensionless parameter δ/σ. (For simplicity, we consider here only the special case in which the well and barrier have equal widths and equal amplitudes.)

For the purpose of calculating equilibrium phase coexistence at a given temperature in the canonical ensemble, the relevant theoretical quantity is the Helmholtz free energy F. The free energy of the highly non-uniform solid phase is determined here within the framework of classical density-functional (DF) theory [20]. The DF approach is based on the existence of a functional $\mathcal{F}[\rho]$ of the spatially varying one-particle density $\rho(\boldsymbol{r})$ that is a minimum [21, 22], under the constraint of fixed average density, at the equilibrium density $\rho_{eq}(\boldsymbol{r})$, where it is equal to the Helmholtz free energy: $\mathcal{F}[\rho_{eq}] = F$.

The free-energy functional $\mathcal{F}[\rho]$ separates naturally into an ideal-gas term $\mathcal{F}_{id}[\rho]$, corresponding to the non-uniform system in the absence of interactions, and an excess term $\mathcal{F}_{ex}[\rho]$, depending entirely upon internal interactions:

$$\mathcal{F}[\rho] = \mathcal{F}_{id}[\rho] + \mathcal{F}_{ex}[\rho]. \tag{2}$$

The ideal-gas free-energy functional is given exactly by

$$\mathcal{F}_{id}[\rho] = k_B T \int \mathrm{d}\boldsymbol{r}\ \rho(\boldsymbol{r})[\ln(\rho(\boldsymbol{r})\Lambda^3) - 1] \tag{3}$$

where $\beta \equiv 1/k_B T$ and Λ is the thermal de Broglie wavelength. In contrast, the excess free-energy functional is in general not known exactly. The theoretical challenge is thus to sensibly approximate $\mathcal{F}_{ex}[\rho]$, and the numerical task then to minimize $\mathcal{F}[\rho]$ with respect to $\rho(\boldsymbol{r})$.

For systems characterized by steeply repulsive short-range interactions and relatively weak longer-range interactions, approximations are greatly facilitated by appeal to thermodynamic perturbation theory [23, 24]. In the case of a pair potential that includes a hard core, such as that of equation (1), perturbation theory is especially appropriate, for then $\phi(r)$ decomposes naturally into a hard-sphere (HS) reference potential $\phi_{HS}(r)$ and a residual perturbation potential $\phi_p(r)$. The free-energy functional is then formally expressed in the form [23]

$$\beta\mathcal{F}[\rho] = \beta\mathcal{F}_{HS}[\rho] + \beta \int_0^1 \mathrm{d}\lambda\ \langle \Phi_p \rangle_\lambda \tag{4}$$

where

$$\Phi_p \equiv \sum_{i<j} \phi_p(|\boldsymbol{r}_i - \boldsymbol{r}_j|) \tag{5}$$

is the total perturbation energy and $\langle\cdots\rangle_\lambda$ denotes an average with respect to the probability distribution of a system whose pair potential is $\phi_\lambda(r) = \phi_{HS}(r) + \lambda\phi_p(r)$. Expansion of $\langle\Phi_p\rangle_\lambda$ about the HS reference system ($\lambda = 0$) generates an exact perturbation series. To first order in the perturbation potential,

$$\beta\mathcal{F}[\rho] \simeq \beta\mathcal{F}_{HS}[\rho] + \frac{1}{2}\int \mathrm{d}\boldsymbol{r} \int \mathrm{d}\boldsymbol{r}'\ \rho(\boldsymbol{r})\rho(\boldsymbol{r}')g_{HS}(\boldsymbol{r},\boldsymbol{r}';[\rho])\beta\phi_p(|\boldsymbol{r}-\boldsymbol{r}'|) \tag{6}$$

where $\mathcal{F}_{HS}[\rho]$ and $g_{HS}(\boldsymbol{r},\boldsymbol{r}';[\rho])$ denote the free-energy and pair distribution functionals, respectively, of the HS solid. With a HS reference system, the exact perturbation expansion amounts to a Taylor series in the inverse temperature with coefficients depending only on density. Evidently the purely entropic zeroth-order term is independent of T and the first-order perturbation term proportional to $1/T$. The neglected higher-order terms are proportional to successively higher powers of $1/T$ with coefficients related to mean fluctuations of the total perturbation energy. Convergence of the expansion is governed by the amplitude of these fluctuations relative to the thermal energy k_BT [23, 25].

Clearly the accuracy of the simple first-order perturbation approximation (equation (6)) must suffer with decreasing temperature. In general though, we can expect considerably higher accuracy for the dense solid than for the fluid. The essential reason for this is the relatively weak variation of the solid two-particle density $\rho(\boldsymbol{r})\rho(\boldsymbol{r}')g_{HS}(\boldsymbol{r},\boldsymbol{r}';[\rho])$ near the sharp step in $\phi_p(r)$ compared with that of its fluid counterpart $\rho^2 g_{HS}(r)$, giving rise to generally smaller fluctuations of Φ_p in the solid than in the fluid. (An exception occurs, however, at an average solid density for which the nearest-neighbour distance is near the step in $\phi_p(r)$.)

A quantitative measure of the accuracy of equation (6) can be drawn from the molecular dynamics simulations of Young and Alder [6], who explicitly computed the first three terms in the perturbation expansion for the related square-shoulder (inverted square-well) system. Over a range of shoulder widths, Young and Alder found the second-order term to be negligible in the dense solid but increasingly significant with decreasing density, the second-order coefficient approaching ~10% of the first-order coefficient near melting. Also worth noting are the Monte Carlo simulations of Weis [27], showing the first-order approximation to be accurate to better than 1% for the Lennard-Jones solid near the triple point. As a rule, we anticipate equation (6) to be valid for the pair potential of equation (1) for $k_BT > \varepsilon$.

Turning now to the excess free-energy functional of the HS reference solid in equation (6), we use the modified weighted-density approximation (MWDA) [26], which provides a reasonably accurate description of the excess entropy of hard-particle solids with minimal computational effort. This maps the excess free energy of the HS solid onto that of the corresponding uniform fluid, according to

$$\mathcal{F}_{ex}^{MWDA}[\rho] = Nf_{HS}(\hat{\rho}) \tag{7}$$

where $N = \int \mathrm{d}\boldsymbol{r}\ \rho(\boldsymbol{r})$ is the number of particles and $f_{HS}(\hat{\rho})$ is the excess free energy per particle of the uniform HS fluid evaluated at an effective or weighted density

$$\hat{\rho} \equiv \frac{1}{N}\int \mathrm{d}\boldsymbol{r} \int \mathrm{d}\boldsymbol{r}'\ \rho(\boldsymbol{r})\rho(\boldsymbol{r}')w(|\boldsymbol{r}-\boldsymbol{r}'|;\hat{\rho}) \tag{8}$$

defined as a weighted average of the physical density with respect to a weight function $w(r)$. The weight function is in turn specified by the requirement

$$\left(\frac{\delta^2\mathcal{F}_{ex}^{MWDA}[\rho]}{\delta\rho(\boldsymbol{r})\,\delta\rho(\boldsymbol{r}')}\right)_{\rho(\boldsymbol{r})\to\rho} = -k_BTc_{HS}^{(2)}(|\boldsymbol{r}-\boldsymbol{r}'|;\rho) \tag{9}$$

ensuring that the approximate functional possesses the correct range of non-locality and generates the exact two-particle Ornstein–Zernike direct correlation function $c^{(2)}_{HS}(|\boldsymbol{r}-\boldsymbol{r}'|;\rho)$ of the HS fluid (see [26] for details). The fluid-state input functions f_{HS} and $c^{(2)}_{HS}$ are taken here from the analytic solution of the Percus–Yevick equation for hard spheres [23].

The perturbation term in equation (6) involves the HS pair distribution functional $g_{HS}(\boldsymbol{r},\boldsymbol{r}';[\rho])$. Aside from parametrizations of its spherical average [27–29], little is known about the detailed form of this functional. On general physical grounds, however, it is expected to be considerably less structured than the fluid function $g_{HS}(|\boldsymbol{r}-\boldsymbol{r}'|;\rho)$. The reason for this is that particles in the dense solid, localized as they are about lattice sites, are much more weakly correlated with their neighbours than in the disordered fluid. This is borne out by the MWDA and related approximations [30–33], all of which map the solid onto an effective fluid whose density $\hat{\rho}$ is found to be much lower than the average solid density. Therefore, as in our earlier study of the square-shoulder system [8], we approximate $g_{HS}(\boldsymbol{r},\boldsymbol{r}')$ by the unit step function of range σ:

$$u(|\boldsymbol{r}-\boldsymbol{r}'|)=\begin{cases}0 & |\boldsymbol{r}-\boldsymbol{r}'|<\sigma\\ 1 & |\boldsymbol{r}-\boldsymbol{r}'|>\sigma.\end{cases} \tag{10}$$

This mean-field approximation, although appropriately excluding correlation of a particle with itself, neglects most of the pair correlations. It should become increasingly realistic, however, upon approach to close packing, as $\rho(\boldsymbol{r})$ tends to a δ-function and the uncorrelated cell (or free-volume) model becomes exact [34]. Recently an alternative perturbation theory based on the spherical average of $g_{HS}(\boldsymbol{r},\boldsymbol{r}';[\rho])$ has been proposed and applied to Lennard-Jones and square-well systems with promising results [35].

For the close-packed solids of interest here, the density distribution is quite reasonably parametrized by the isotropic Gaussian *ansatz*

$$\rho(\boldsymbol{r})=\left(\frac{\alpha}{\pi}\right)^{3/2}\sum_{\boldsymbol{R}}\mathrm{e}^{-\alpha|\boldsymbol{r}-\boldsymbol{R}|^2} \tag{11}$$

which places a normalized Gaussian at each lattice site $\boldsymbol{R}$ of the close-packed fcc crystal. For $\alpha\sigma^2>50$, the ideal-gas free-energy functional per particle (equation (3)) is very accurately approximated by

$$\beta\mathcal{F}_{id}/N=\frac{3}{2}\ln(\alpha/\pi)-\frac{5}{2}. \tag{12}$$

Combining equations (6), (7), (10), and (12), our approximate total free-energy functional per particle is given by

$$\beta\mathcal{F}[\rho]/N=\frac{3}{2}\ln(\alpha/\pi)-\frac{5}{2}+\beta f_{HS}(\hat{\rho})+\frac{1}{2N}\int\mathrm{d}\boldsymbol{r}\int\mathrm{d}\boldsymbol{r}'\;\rho(\boldsymbol{r})\rho(\boldsymbol{r}')u(|\boldsymbol{r}-\boldsymbol{r}'|)\beta\phi_p(|\boldsymbol{r}-\boldsymbol{r}'|). \tag{13}$$

Minimization of $\mathcal{F}[\rho]$ with respect to the single variational width parameter α at fixed average ρ determines the free energy of the solid.

For the fluid phase we take the uniform (constant-ρ) limit of equation (6):

$$\beta F(\rho)/N\simeq\ln(\rho)-1+\beta f_{HS}(\rho)+2\beta\pi\rho\int_0^\infty\mathrm{d}r\;r^2g_{HS}(r;\rho)\phi_p(r) \tag{14}$$

together with the essentially exact Carnahan–Starling and Verlet–Weis expressions [23] for the fluid functions $f_{HS}(\rho)$ and $g_{HS}(r;\rho)$, respectively. This ensures that the fluid and solid phases are treated within the same perturbation approximation, which is essential for

a consistent description of the fluid–solid transition. We stress, however, that the first-order perturbation approximation is expected to be of more limited validity for the fluid than for the solid.

In practice, the fluid and solid free energies per volume F/V are computed as a function of reduced average density $\rho\sigma^3$ at a given reduced temperature k_BT/ε. For hard spheres alone, F/V is simply a monotonically increasing function of ρ. The addition of a square well or barrier of width δ induces inflection in the curve of F/V versus ρ, which, for sufficiently narrow width ($\delta \ll \sigma$) and low T, may lead to coexistence between an expanded (lower-density) solid and a condensed (higher-density) solid. The densities of coexisting fluid and solid phases are established by means of a Maxwell common-tangent construction on the fluid and solid F/V, or equivalently an equal-area construction on the chemical potential $\mu = \partial(F/V)/\partial\rho$, ensuring equality of the chemical potentials and pressures in the two phases. Repetition of the procedure for a range of temperatures systematically maps out the fluid–solid–solid coexistence region in the T–ρ plane.

In addition to the free energy, density-functional theory also predicts the form of the density distribution. Within the Gaussian approximation (equation (11)), this amounts to a prediction of the width parameter α, which gauges the degree of particle localization. A more convenient measure of localization is the Lindemann ratio L, defined as the ratio of the rms particle displacement to the equilibrium nearest-neighbour distance in the solid. For an fcc crystal of average density ρ, $L = \sqrt{(3/\alpha)}/a$, where $a = (4/\rho)^{1/3}$ is the lattice constant. Although the Lindemann ratio is often considered only along the melting curve, in this paper we examine L in the solid at fixed density away from melting.

2.2. Monte Carlo simulation

To test our theoretical predictions for the Lindemann ratio, we have independently performed a series of Monte Carlo (MC) simulations, implementing the standard Metropolis algorithm for a perfect fcc crystal at fixed temperature and density in a cubic simulation cell with periodic boundary conditions. A collection of N particles, interacting via the pair potential $\phi(r)$, and initially positioned at fcc lattice sites, are subjected sequentially to a series of trial moves of randomly chosen direction and amplitude. The maximum amplitude of trial moves is chosen to permit an acceptance ratio of $\sim$0.4. A move that changes the internal energy by an amount ΔU is automatically accepted if $\Delta U < 0$. If $\Delta U > 0$, the move is accepted only with probability $\exp(-\Delta U/k_BT)$. Following each accepted move, the positions of all particles are adjusted to maintain a fixed centre of mass. This adjustment is essential to avoid gradual drifting of the lattice sites. After an equilibration stage of 10^4 trial moves per particle, statistics on rms displacements of the particles from their lattice sites are accumulated over a further 5×10^4 trial moves. Finite-size effects are monitored by simulating systems of various sizes. All results reported here are for systems of $N = 16\,384$ particles, for which finite-size effects are negligible.

3. Results and discussion

We have applied the approach described in section 2 to a hard-core system interacting via the square-well–barrier model pair potential of equation (1). To assess the influence of individual features of the pair potential on phase behaviour, we have also examined hard-core systems interacting via square-well and square-barrier potentials alone (lines 2 and 3, respectively, of equation (1)). As noted in section 1, the square-well and square-well–barrier potentials may roughly model interactions in colloidal systems. Furthermore, the square-

Table 1. Monte Carlo simulation data of figures 2–4(b) for square-well (SW), square-barrier (SB), and square-well–barrier (SWB) solids with $\delta/\sigma = 0.06$: the Lindemann ratio L as a function of reduced temperature $t = k_B T/\varepsilon$ at reduced solid densities $\rho\sigma^3 = 1.092$ and 1.294, corresponding to nearest-neighbour distances $r_{nn}/\sigma = 1.09$ and 1.03, respectively.

		L	
	t	$\rho\sigma^3 = 1.092$	$\rho\sigma^3 = 1.294$
SW			
	1.9	0.1196 ± 0.0006	$0.029\,16 \pm 0.000\,09$
	2.0	0.1184 ± 0.0009	$0.029\,33 \pm 0.000\,07$
	2.1	0.1172 ± 0.0004	$0.029\,45 \pm 0.000\,05$
	2.2	0.1169 ± 0.0005	$0.029\,65 \pm 0.000\,06$
	2.3	0.1163 ± 0.0004	$0.029\,77 \pm 0.000\,09$
	2.4	0.1155 ± 0.0005	$0.029\,86 \pm 0.000\,10$
SB			
	2.0	0.1181 ± 0.0005	$0.029\,32 \pm 0.000\,08$
	2.2	0.1162 ± 0.0006	$0.029\,65 \pm 0.000\,09$
	2.4	0.1156 ± 0.0005	$0.029\,85 \pm 0.000\,07$
	2.6	0.1146 ± 0.0006	$0.030\,13 \pm 0.000\,08$
	2.8	0.1137 ± 0.0007	$0.030\,31 \pm 0.000\,10$
	3.0	0.1130 ± 0.0007	$0.030\,43 \pm 0.000\,08$
	3.2	0.1125 ± 0.0005	$0.030\,57 \pm 0.000\,11$
	3.4	0.1118 ± 0.0004	$0.030\,67 \pm 0.000\,07$
	3.6	0.1112 ± 0.0003	$0.030\,75 \pm 0.000\,09$
	3.8	0.1107 ± 0.0004	$0.030\,89 \pm 0.000\,07$
SWB			
	3.0	0.1229 ± 0.0008	$0.028\,39 \pm 0.000\,08$
	3.5	0.1199 ± 0.0006	$0.028\,95 \pm 0.000\,05$
	4.0	0.1176 ± 0.0006	$0.029\,37 \pm 0.000\,07$
	4.5	0.1164 ± 0.0007	$0.029\,67 \pm 0.000\,08$
	5.0	0.1149 ± 0.0006	$0.029\,98 \pm 0.000\,10$
	5.5	0.1142 ± 0.0006	$0.030\,19 \pm 0.000\,08$
	6.0	0.1128 ± 0.0003	$0.030\,40 \pm 0.000\,05$

barrier potential may be of relevance to certain simple metals (e.g. Al) whose effective pair potentials exhibit a barrier.

Detailed predictions of the theory are presented in figures 2–4. Part (a) of each figure displays the predicted T–ρ phase diagram for the case where $\delta/\sigma = 0.06$. This case is of particular relevance as it defines the predicted threshold for stability of the coexistence between isostructural solids in the square-well system [36]. Whereas for $\delta/\sigma < 0.06$ the fluid–solid–solid triple point lies below the critical temperature, permitting a stable solid–solid transition over a finite temperature range, for $\delta/\sigma > 0.06$ the transition is pre-empted at all T by the fluid–solid transition. Note that such a narrow well is insufficient to induce a vapour–liquid transition, resulting in the appearance of only a single fluid phase. Part (b) of each figure shows the predicted Lindemann ratio as a function of temperature, up to the critical temperature, at fixed average densities $\rho\sigma^3 = 1.092$ and 1.294. These densities are of special interest as they correspond to the fcc equilibrium nearest-neighbour distances $r_{nn}/\sigma = 1.09$ (barrier centre) and 1.03 (well centre), respectively. Corresponding MC simulation results are plotted for comparison and tabulated in table 1. For reference, the MC results for the HS solid ($T \to \infty$) are $L = 0.1024 \pm 0.0003$ and $L = 0.032\,67 \pm 0.000\,09$ at the lower and higher densities, respectively. Below, we discuss first the phase diagrams

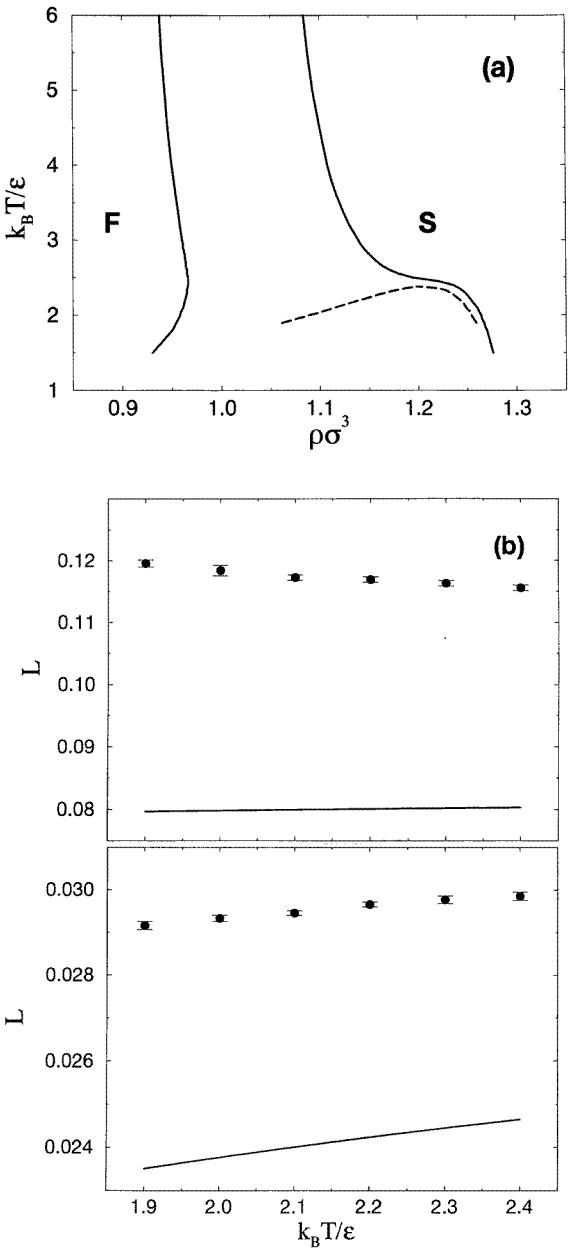

Figure 2. The square-well system with well width $\delta/\sigma = 0.06$. (a) The predicted phase diagram of temperature versus density (reduced units). The full curves represent fluid–solid coexistence, and the dashed curves metastable isostructural (fcc) solid–solid coexistence, which for this value of δ/σ is pre-empted by fluid–solid coexistence (see the text). The regions of fluid (F) and solid (S) stability are labelled. (b) The Lindemann ratio versus reduced temperature at fixed average density $\rho\sigma^3 = 1.092$, or nearest-neighbour distance $r_{nn}/\sigma = 1.09$ (upper panel), and $\rho\sigma^3 = 1.294$, or $r_{nn}/\sigma = 1.03$ (lower panel). The curves represent theoretical predictions, the symbols the corresponding Monte Carlo simulation results. Note the change of scale between the upper and lower panels.

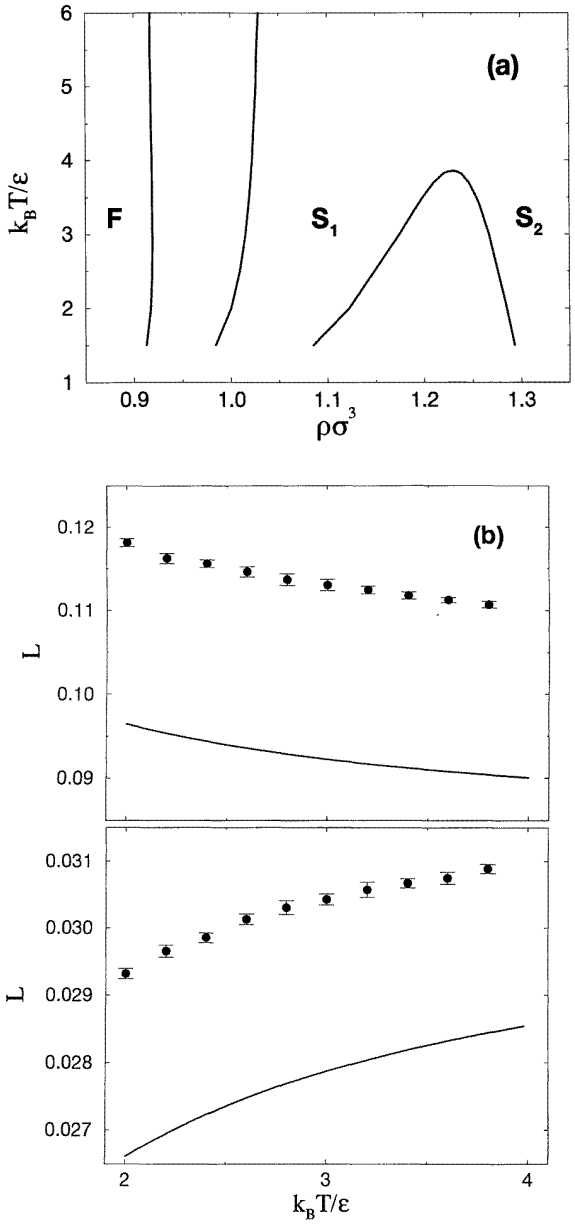

Figure 3. The square-barrier system with barrier width and separation $\delta/\sigma = 0.06$, with the same format as figure 2. (a) The predicted phase diagram, exhibiting now stable isostructural (fcc) solid–solid coexistence. Regions of fluid (F), expanded solid (S_1), and condensed solid (S_2) stability are labelled. (b) The Lindemann ratio, exhibiting anomalous increase of particle localization with increasing temperature at density $\rho\sigma^3 = 1.092$ (upper panel).

and then the Lindemann ratios.

In the high-temperature limit ($T \gg \varepsilon/k_B$) all three systems are dominated by the hard-core interaction. The fluid–solid coexistence curves therefore tend to the vertical at

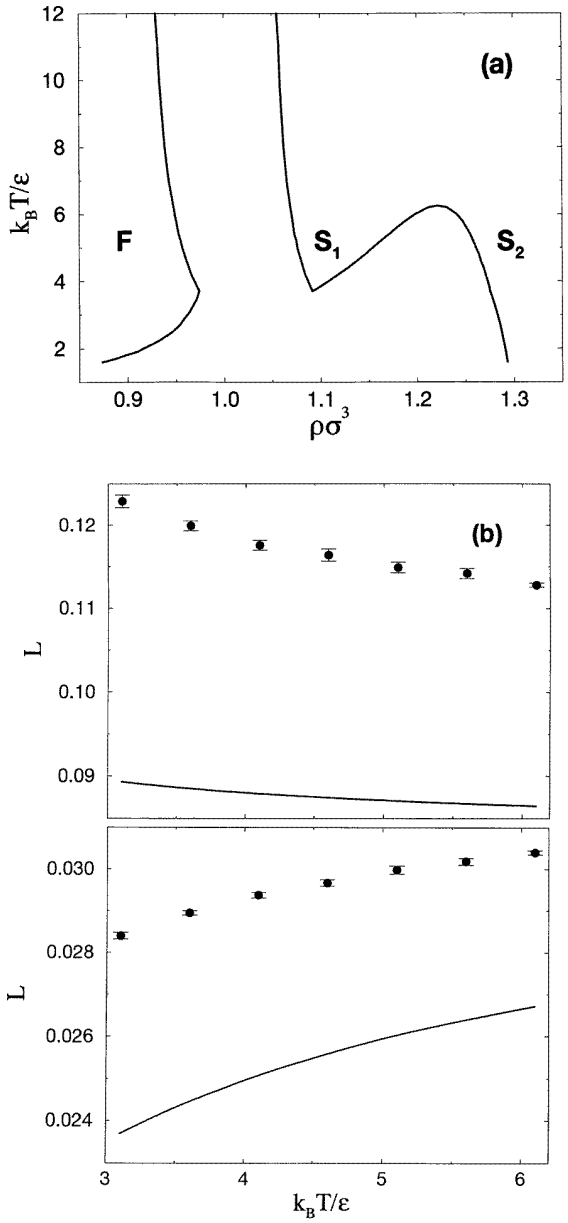

Figure 4. The square-well–barrier system with well and barrier width $\delta/\sigma = 0.06$, with the same format as figure 2. (a) The predicted phase diagram, exhibiting stable isostructural (fcc) solid–solid coexistence. (b) The Lindemann ratio, exhibiting anomalous T-dependence at density $\rho\sigma^3 = 1.092$ (upper panel).

the predicted HS fluid and solid freezing densities $\rho_f\sigma^3 = 0.912$ and $\rho_s\sigma^3 = 1.044$ (for comparison, the simulation values [1] are 0.94 and 1.04). In the opposite low-temperature limit ($T \ll \varepsilon/k_B$), perturbation theory inevitably breaks down, as discussed in section 2. For this reason, we have conservatively restricted our calculations to $k_BT/\varepsilon > 1.5$. Nevertheless,

the $T = 0$ limit in each case is intuitively clear. In the square-well and square-well–barrier systems (figures 2(a) and 4(a)) the solid wins energetically over the fluid as $T \to 0$ (or equivalently $\varepsilon \to \infty$). The ground state must be coexistence between a zero-density fluid (vacuum) and a condensed solid of density $\rho_s\sigma^3 = 1.294$ ($r_{nn}/\sigma = 1.03$). Strictly viewed, of course, all solids for which r_{nn} lies within the well (but beyond the core) are degenerate precisely *at* $T = 0$. At finite but infinitesimally low T, however, entropy breaks this degeneracy. Free-volume considerations then dictate that r_{nn} at the centre of the well maximizes the entropy. The square-barrier system develops a second hard core at range $\sigma' \equiv \sigma + 2\delta = 1.12$ as $T \to 0$. Since there is no energetic advantage of the solid over the fluid, the ground state is rather a coexistence between a fluid and an expanded solid of large hard spheres of diameter σ', at densities $\rho_f\sigma^3 = 0.912(\sigma/\sigma')^3 = 0.649$ and $\rho_{s1}\sigma^3 = 1.044(\sigma/\sigma')^3 = 0.743$, and a condensed solid of small hard spheres at density $\rho_{s2}\sigma^3 = 1.294$. We do not consider here the possible stability of crystal structures other than fcc, which are not expected to bear on the stability of isostructural solid–solid transitions. It should be noted, however, that Rascón *et al* [11], using a similar theoretical approach, have recently found evidence for stable bcc crystals in square-shoulder systems with sufficiently wide shoulders at intermediate densities and temperatures.

Comparing the phase diagrams in figures 2–4, one observes that the stability of solid–solid coexistence, relative to fluid–solid coexistence, for the square-well potential is significantly *enhanced* by addition of a square barrier. The solid–solid reduced critical temperature $t_c \equiv k_B T_c/\varepsilon$ increases from $t_c = 2.4$ for the square-well system (metastable), through $t_c = 3.9$ for the square-barrier system, to $t_c = 6.3$ for the combined square-well–barrier system. The latter may be compared with a fluid–solid–solid reduced triple-point temperature of $t_t = 3.7$. The enhancement can be intuitively understood by considering independently the role of different features of the pair potential in inducing inflection in the free energy per volume. The square well acts to reduce F/V at high densities corresponding roughly to $r_{nn} \simeq \sigma + \delta$. The square barrier, in contrast, augments F/V at lower densities where $r_{nn} \simeq \sigma + 2\delta$. The net effect is a *constructive* superposition that increases the total inflection and helps to stabilize solid–solid coexistence.

What relevance, if any, might exist between the curious phase behaviour predicted for these model systems and that of real colloidal suspensions? As mentioned in section 1, a practical hindrance to experimental observation of solid–solid transitions is polydispersity in the diameter of colloidal particles, which tends to smear out any influence of interactions of range comparable to the spread in size distribution. Although we have not numerically determined the threshold interaction range (δ) for solid–solid stability, it is evidently considerably longer than that for the simple square-well system. This may have important consequences for the observability of solid–solid transitions in colloidal suspensions. Our results suggest optimal likelihood of observing isostructural solid–solid transitions in charge-stabilized suspensions whose interactions exhibit a pronounced barrier and whose polydispersity is limited to a few per cent. Further prerequisites seem to be a Coulomb barrier considerably narrower than the core diameter, implying strong screening (high salt or counter-ion concentration), and steric stabilization against coagulation and gelation.

Finally we discuss the peculiar dependence of the Lindemann ratio on temperature and density. Although the theoretical values of L are consistently low, the predicted trends are, with one exception (see below), qualitatively consistent with simulation. Particularly intriguing is the prediction, confirmed by simulation, that for the square-barrier and square-well–barrier systems at the density $\rho\sigma^3 = 1.092$ (nearest-neighbour lattice site separation $r_{nn}/\sigma = 1.09$), L *decreases* with increasing T. This behaviour challenges common intuition, according to which thermal disorder, and thus rms displacements, increase with T. It is

easily understood, however, by noting that at this density r_{nn} falls directly at the centre of the repulsive barrier. In other words, nearest-neighbour barriers overlap. Suppose first that every particle were localized at its equilibrium (lattice site) position. Each particle would then sit beneath the barrier of every one of its neighbours and pay an energetic price ε for each neighbour. A random displacement that takes a given particle closer to one of its neighbours costs no internal energy—*for a flat barrier*—and may even reduce the internal energy if the displacement takes the particle outside the barriers of its other neighbours. With decreasing T (or equivalently increasing barrier height), such displacements become increasingly favourable energetically, broadening the one-particle density distribution (or increasing L). Qualitatively similar behaviour was predicted in [8] for a dense square-shoulder solid. We have since confirmed this prediction by MC simulation. Like reasoning accounts for the increase of L with T at the higher density $\rho\sigma^3 = 1.294$ ($r_{nn}/\sigma = 1.03$), where nearest-neighbour wells (or gaps for the square-barrier potential) overlap. The single discrepancy between theory and simulation occurs for the square-well system at the lower density (where $r_{nn}/\sigma = 1.09$ lies outside the well). Here theory predicts a very gradual increase of L with T, in qualitative disagreement with simulation (the upper panel of figure 2(b)). The source of this discrepancy is uncertain, but may be related to the fact that in this case the system is in the metastable region of the phase diagram.

4. Conclusions

In summary, we have applied a practical density-functional-perturbation theory to predict the phase behaviour of a system interacting via a model pair potential that includes a hard core and additional short-range attractive and repulsive interactions. The combination of narrow attractive square-well and repulsive square-barrier potentials is predicted to significantly enhance the stability of isostructural solid–solid transitions over that of a square-well potential alone. We conclude that such transitions, if experimentally observable in colloidal suspensions, are most likely to be seen in charge-stabilized suspensions whose interactions include a narrow Coulomb barrier. It is hoped that the present study may help to guide future parametrizations of more realistic interaction models for colloidal systems. Finally, the Lindemann ratio for these idealized systems has been shown, from both theory and Monte Carlo simulation, to decrease upon increasing temperature at densities for which neighbouring barriers overlap. Whether this unusual behaviour is purely an artifact of potentials with sharp steps, or might occur also for some continuous potentials, is a matter for future consideration.

Acknowledgments

We gratefully acknowledge Drs A M Denton and C N Likos for helpful discussions.

References

[1] Alder B J and Wainwright T E 1960 *J. Chem. Phys.* **33** 1439
Hoover W G and Ree F H 1968 *J. Chem. Phys.* **49** 3609
Alder B J, Hoover W G and Young D A 1968 *J. Chem. Phys.* **49** 3688
Young D A and Alder B J 1974 *J. Chem. Phys.* **60** 1254
[2] Pusey P N 1991 *Liquids, Freezing and Glass Transition* ed J-P Hansen, D Levesque and J Zinn-Justin (Amsterdam: North-Holland)
[3] Bolhuis P and Frenkel D 1994 *Phys. Rev. Lett.* **72** 2211

Bolhuis P and Frenkel D 1995 *Phys. Rev.* E **50** 4880
[4] Likos C N, Németh Zs T and Löwen H 1994 *J. Phys.: Condens. Matter* **6** 10 965
[5] Kincaid J M, Stell G and Goldmark E 1976 *J. Chem. Phys.* **65** 2172
[6] Young D A and Alder B J 1979 *J. Chem. Phys.* **70** 473
[7] Bolhuis P and Frenkel D 1997 *J. Phys.: Condens. Matter* **9** 381
[8] Denton A R and Löwen H 1997 *J. Phys.: Condens. Matter* **9** L1
[9] Rascón C, Velasco E, Mederos L and Navascués G 1997 *J. Chem. Phys.* **106** 6689
[10] Németh Zs T and Likos C N 1995 *J. Phys.: Condens. Matter* **7** L537
Likos C N and Senatore G 1995 *J. Phys.: Condens. Matter* **7** 6797
[11] Rascón C, Mederos L and Navascués G 1995 *J. Chem. Phys.* **103** 9795
[12] Tejero C F, Daanoun A, Lekkerkerker H N W and Baus M 1994 *Phys. Rev. Lett.* **73** 752
Tejero C F, Daanoun A, Lekkerkerker H N W and Baus M 1995 *Phys. Rev.* E **51** 558
[13] Hecht C E and Lind J 1976 *J. Chem. Phys.* **64** 641
[14] The critical exponents have been shown to be mean-field ones in the absence of defects:
Chou T and Nelson D R 1996 *Phys. Rev.* E **53** 2560
[15] Barrat J L and Hansen J-P 1986 *J. Physique* **47** 1547
[16] Bolhuis P G and Kofke D A 1996 *Phys. Rev.* E **54** 634
[17] Verduin H and Dhont J K G 1994 *J. Colloid Interface Sci.* **172** 425
[18] Verwey E J W and Overbeek J T G 1948 *Theory of the Stability of Lyophobic Colloids* (Amsterdam: Elsevier)
[19] In practice, a steep core repulsion, stabilizing the suspension against coagulation, may be achieved by surface treatment of the macroions, e.g. polymer adsorption.
[20] Evans R 1992 *Inhomogeneous Fluids* ed D Henderson (New York: Dekker)
Oxtoby D W 1990 *Liquids, Freezing and Glass Transition (Les Houches Session 51)* ed J-P Hansen, D Levesque and J Zinn-Justin (New York: Elsevier)
Singh Y 1991 *Phys. Rep.* **207** 351
Löwen H 1994 *Phys. Rep.* **237** 249
[21] Mermin N D 1965 *Phys. Rev.* **137** A1441
[22] Evans R 1979 *Adv. Phys.* **28** 143
[23] Hansen J-P and McDonald I R 1986 *Theory of Simple Liquids* 2nd edn (London: Academic)
[24] Weeks J D, Chandler D and Andersen H C 1971 *J. Chem. Phys.* **54** 5237
Andersen H C, Chandler D and Weeks J D 1976 *Adv. Chem. Phys.* **34** 105
[25] Zwanzig R 1954 *J. Chem. Phys.* **22** 1420
[26] Denton A R and Ashcroft N W 1989 *Phys. Rev.* A **39** 4701
Denton A R and Ashcroft N W 1991 *Phys. Rev.* A **42** 7312
[27] Weis J-J 1974 *Mol. Phys.* **28** 187
[28] Kincaid J M and Weis J-J 1977 *Mol. Phys.* **34** 931
[29] Rascón C, Mederos L and Navascués G 1996 *Phys. Rev.* E **54** 1261
[30] Tarazona P 1984 *Mol. Phys.* **52** 81
Tarazona P 1985 *Phys. Rev.* A **31** 2672
[31] Curtin W A and Ashcroft N W 1985 *Phys. Rev.* A **32** 2909
Curtin W A and Ashcroft N W 1986 *Phys. Rev. Lett.* **56** 2775
[32] Lutsko J F and Baus M 1990 *Phys. Rev. Lett.* **64** 761
Lutsko J F and Baus M 1990 *Phys. Rev.* A **41** 6647
[33] Likos C N and Ashcroft N W 1992 *Phys. Rev. Lett.* **69** 316 (erratum **69** 3134)
[34] Tejero C F, Ripoll M S and Pérez A 1995 *Phys. Rev.* E **52** 3632
[35] Rascón C, Mederos L and Navascués G 1996 *Phys. Rev. Lett.* **77** 2249
[36] The estimate here of the threshold $\delta/\sigma \simeq 0.06$ for stability of isostructural solid–solid coexistence in the square-well system differs slightly from that of reference [4] because of the use here of the Verlet–Weis $g_{HS}(r)$ (as opposed to the Percus–Yevick form) in computing the free energy of the fluid phase.